DIFFERENTIATION OF NEURAL STEM CELL USING SMALL MOLECULES IN 2D AND 3D CULTURE SYSTEM

A Thesis
Submitted to
the Temple University Graduate Board

In Partial Fulfillment
of the Requirements for the Degree
MASTER OF SCIENCE

---

by
Xinglong Shi
December 2015

Examining Committee Members:

Dr. Won H. Suh, Thesis Advisor, Temple U., Bioengineering
Dr. Cezary Marcinkiewicz, Committee Chair, Temple U., Bioengineering
Dr. Philip Lazarovici, External Member, School of Pharmacy- Institute for Drug Research

ABSTRACT

The neuronal differentiation of neural stem cells (NSCs) has received much attention due to its potential for the treatment of neurodegenerative diseases (i.e., Parkinson's and Alzheimer's diseases). In this regard, discovering compounds that direct differentiation of NSCs is highly required to facilitate therapeutic applications. In this study, we examined various bioactive compounds (SA1, SA2, LiCl, Compound B, and DHED) to induce the neuronal differentiation of human neural stem cells (hNSCs). The study was conducted on the cells grown in three dimensional (3D) hydrogel or two dimensional (2D) environment since 3D hydrogel mimics the extracellular matrix and provide physiologically more relevant environment than 2D cell culture system. Three-dimensional (3D) hydrogel systems in this study involve polysaccharides such as alginate and hyaluronic acid. Neuronal differentiation of hNSCs was monitored in genetic level and protein level by quantitative reverse transcription polymerase chain reaction (RT-qPCR) and immunocytochemistry (ICC), respectively. This study will show the effect of bioactive compounds on hNSCs differentiation in 2D and 3D culture system.

I dedicate my thesis work to my family

for all their sacrifices and support

for me to be where I am today.

I also dedicate this thesis to my many friends who have

supported me throughout the process.

ACKNOWLEDGMENTS

I would like to thank Dr. Won H. Suh for providing me with research guidance and funding required for this project, and all the members of the Dr. Suh lab for their individual contributions. I thank my thesis committee members Dr. Cezary Marcinkiewicz, and Dr. Philip Lazarovici for their invaluable feedback and guidance. I also thank Dr. Cynthia Bergman from Fox Chase Cancer Center for help with Mass spectrometry data collection.

TABLE OF CONTENTS

LIST OF FIGURES

CHAPTER 1: INTRODUCTION

Stem Cell Therapies and Molecular Approaches

Stem cell therapy has been seen thought as a promising method to restore functional losses caused by aging, injury, and/or disease processes - especially in the brain - such as Alzheimer's and Parkinson's diseases, two most prevalent aged-related diseases. For example, Parkinson's disease (PD), the second most common neurodegenerative disorder in America and the most common one around the world, is caused by the dysfunction and function loss of dopaminergic cells in the brain, which ultimately results in the shortage of dopamine molecules [1]. The decrease of dopamine in the brain can eventually lead a person suffering from PD.

Neurons, generally, do not divide in the central nerve systems (CNS), so new dopaminergic cells cannot be generated by the CNS itself. Current existing therapies for the PD include levodopa, dopamine agonists, and surgeries but they only relieve some of the symptoms and/or slow down the deterioration process since these therapies only focus on providing the dopamine temporarily and not permanently. What is worse, the longtime use of current drugs will cause certain side effects, such as the levodopa-related motor complications. The complications can cause fluctuations, dyskinesia and dystonia. These side effects are very hard to treat and can be very disabling [2]. Under this premises, the development of stem cell therapy can provide an alternative permanent solution for the treatment of the Parkinson's disease and other similar neurodegenerative diseases.

Stem cell therapy is a technique that replaces aged, damages, and/or diseased cells with newly generated cells derived from various stem cell sources. The stem cells are undifferentiated cells that are capable of self-renewing and differentiating into other somatic cell types including neurons, oligodendrocytes, and astrocytes. There are many stem cell sources including embryonic stem cells, adult stem cells, and induced pluripotent stem cells [3, 4]. Embryonic stem cells are pluripotent stem cells while adult stem cells are multi-potent stem cells. The obstacles involving stem cell-based therapies are that the molecular regulations of each stem cells are very complicated and dynamic microenvironments, in addition, influence their differentiation processes. In regard to transplantation (studies), the differentiated cells should not only survive long-term but also will need to functionally integrate into the host living system after injection (or incorporation). Such difficult-to-predict situations act as a deterrence for stem cell-based therapies to work in a clinical setting.

One desirable stem cell source for brain-related diseases and injuries is neural stem cells. Neural stem cell (NSC) - a multi-potent adult stem cell - originates from the central nervous system (CNS). NSCs can differentiate into neurons, astrocytes and oligodendrocytes. The differentiation of NSCs is regulated by the exogenous stimuli from the brain microenvironment and the various molecules being presented to them during the various regulation processes. Different stimuli will trigger different signaling pathways in NSCs and lead to a terminally differentiated cell.

Multiple molecules have been investigated to induce the neuronal differentiation of neural stem cells such as peptides and small molecules [5, 6]. Small molecules, for instance, can target various endogenous signaling pathways and regulate the self-renewal and differentiation processes. Small molecules are normally smaller than 1000 Daltons. The small sub-nanometer size allows for several advantages over other materials [6]:

1. Hydrophobicity and functionality-controlled small molecules can enter cells and target the downstream cellular pathways without extra modifications.
2. Small molecules are generally synthesized via organic chemistry approaches so no animal products are involved and they are chemically well-defined.
3. The concentration of small molecules can be precisely controlled since their purity, solubility and optical properties are well-defined.

These physicochemical and biological properties render certain small molecules to be optimal regulators in modulating various stem cell sources to differentiate, specifically.

In the experiments that will be described throughout this thesis work, dehydroevodiamine HCl (DHED), LiCl, compound B, retinoic acid (RA) peptide amphiphile (SA1) and palmitic acid peptide amphiphile (SA2) were chosen as molecules that can potentially regulate neural stem cell differentiation processes. ReNCell VM (RVM; Millipore, Inc.)   An immortalized human neural progenitor cell line from the mesencephalon of a fetal brain - was treated with the abovementioned small molecules in specific concentrations based on cytotoxicity assays. The differentiation levels were measured by real-time reverse transcriptase quantitative PCR (RT-qPCR) and immunocytochemistry (ICC).

Lithium (Li^+) is a well-known psychiatric medication and a GSK-3β inhibitor, and it is also described as being neuroprotective based on its anti-inflammatory effects [7]. Lithium is thought to be involved in the Wnt/β-catenin pathway via the inhibitory activity over the GSK-3β protein. The effect and mechanism of lithium on the neuronal differentiation of NSCs are still not well-defined. One theory is that the inhibition of GSK-3β will lead to the stabilization of β-catenin in the cells. The stabilized β-catenin can enter the nucleus and bind to T-cell factor/lymphoid enhancer binding factor (TCF/LEF) transcription factor, which finally activates transcription of Wnt target genes. The activated genes are highly related to the neuronal differentiation [8-10]. Furthermore, based on Car Jamieson's article, LiCl can stimulate the nuclear retention of β-catenin, which means more β-catenin can be retained in the nuclear [11].

Peptide Amphiphiles: Retinoic acid is a widely utilized molecule that induces neuronal differentiation in stem cells. Based on the Mijeong Kim, Kaomei Guan, Bo-Tao Tan's articles, RA is capable of inducing the differentiation of embryonic stem cells (ESCs) into neurons *in vitro* [12-14]. For example, RA molecules were applied at 0.1~1 μM concentrations to early stage ESCs that resulted in neuronal differentiations. The effect of RA molecules on NSCs to differentiate are difficult to define sometimes due to the toxicity of RA. The Suh lab has developed a new cell penetrating peptide system (PepB) for the delivery of bioactive compounds such as RA that circumvents the original lipid's toxicity as well as its cell incorporation issues. This thesis work will show some results of PepB conjugated with bioactive lipids. Due to patent-related issues the chemical components cannot be revealed and they will be designated as synthetic agent 1 incorporating retinoic acid (SA1) and synthetic agent 2 incorporating palmitic acid (SA2) and they are both peptide amphiphiles (PAs).

Dehydroevodiamine HCl (DHED) (kindly provided as a gift from Braintropia, Inc., South Korea). is a component separated from *Evodia rutaecarpa* plant. Most studies about DHED were related to its neuro-protective effect. DHED has been shown to decrease the neuronal death in Alzheimer's rats and can protect against learning and memory impairments tested via Cognitive Disturbance animal models [15, 16]. In addition, DHED can suppress the activation of GSK-3β in the WT/GFX animal models [17]. DHED have not been investigated specifically for NSC differentiation studies. We hypothesize that DHED may have a positive effect on the neuronal differentiation based on its GSK-3β suppression effect.

The last material is the compound B, another plant extract (kindly provided as a gift from Braintropia, Inc., South Korea). The compositions of compound B are unknown. The effect of compound B to the neural stem cells is also unknown, in addition. The use of compound B is more exploratory.

Three-Dimensional (3D) Culture System

The traditional cell culture system and *in vitro* cell biology experiments are culturing mammalian cells on 2-Dimensional (2D) polystyrene flat surfaces (e.g., T75 or well plates) as monolayer cultures. The cell culture experiments generally involve medium changes and the application of specific testing chemicals. 2D cell cultures are very convenient and of high cell viability but the testing results from 2D culture systems have been questioned for their physiological validity as they do not recapitulate the 3D microenvironment, which the cells originated from [18]. The differences of cell morphology, interactions with extracellular matrix (ECM), and cell-to-cell interactions between 2D culture systems and 3D real tissues have been a source of debate. Synthetic 3D cell culture systems are designed for studying the cell growth and associated behavior in the microenvironment mimicking the real tissue. Compared to the 2D culture system, 3D culture system reveals the cell behavior and morphology more accurately to the one in the real tissue.

For example, cells in the 3D culture system are normally elliptical, or round while the cells in 2D culture system spread on the surface and are flat. In addition, the cells in 2D culture systems form single cell layers (monolayers), while the cells in 3D culture system are capable of growing in the shape of multilayers (i.e., 3D structures). Research has also been proved that 3D cell culture systems can influence the cell proliferation, differentiation and migration. Leach and his colleagues found that neural stem cells in 3D collagen culture systems migrated far away from the sphere and spread out longer neurites than in 2D culture system. In addition, they also found that the neuronal differentiation in 3D collagen culture systems is less than in the 2D culture system [19]. Another benefit of 3D culture system is that an appropriate 3D cell culture can reveal drug efficiencies and cytotoxicities identical to testing via animal models [20]. *In vivo* tests are important steps for testing drug efficacy before conducting any clinical trials. Animal tests, however, can incur high costs and are even more time-consuming. A well-developed 3D culture system can potentially reduce the number of initial animal trials and lead to saving more time and effort.

One popular platform for generating synthetic 3D cell culture systems is utilizing crosslinked hydrogel systems. Hydrogel is a three-dimensional polymeric system that incorporates water and cross-links that allow the formation of networked structures. Due to the high water content (>90%), hydrogels can recapitulate the 3D microenvironment of living tissues and are allow researchers to form candidate extracellular matrix (ECM) structures in a facile manner. A variety of building blocks (organic molecules) can be used for the synthesis of hydrogels including peptide amphiphiles, polysaccharides and synthetic (petrofuel-based) polymers. In this thesis study, peptide amphiphiles and polysaccharide-based hydrogels (i.e., alginate and hyaluronate) will be utilized.

CHAPTER 2: SPECIFIC AIMS

In this study, specific bioactive molecules (SA1, SA2, LiCl, DHED, and compound B) were chosen to induce the neuronal differentiation of human neural stem cells (hNSCs). Furthermore, three hydrogel-based 3D culture systems, including peptide amphiphile H_2N--SSSGGK(C16)HHH-C(O)-NH_2 (C_{16}-GSH), alginate, and hyaluronic acid, were synthesized and investigated. Bioactive molecules' effects on the neuronal differentiation processes were investigated in the 3D culture systems. The mRNA of differentiated neural stem cells were collected at multiple time points (i.e., 1 week, 2 weeks) in both 2D and 3D culture systems and were analyzed using real time reverse transcriptase quantitative polymerase chain reaction (RT-qPCR). Gene expression levels of neural stem cell markers Sox 2 and Nestin, neuronal markers β3-tubulin and Map 2, astrocyte marker GFAP, and oligodendrocyte marker OMG were measured. Immunocytochemistry (ICC) staining for neuronal marker β3-tubulin will be quantified via fluorescence microscopy.

In order to achieve the goals mentioned, the following specific aims were established:

1) Cytotoxicity profiling of bioactive molecules (SA1, SA2, LiCl, DHED, compound B).
2) Synthesis and testing of selected 3D culture systems (i.e., PAs, alginate, hyaluronate).
3) Neural stem cell differentiation using bioactive molecules in 2D & 3D culture systems.

Cytotoxicity experiments will be conducted for bioactive molecules to determine the safe concentrations for conducting the differentiation experiments. Biocompatibility, cell encapsulation rate and possibility for performing ICC and RT-qPCR will be tested for the three kinds of hydrogels. A best 3D culture system will be chosen for further neural stem cell differentiation experiments.

CHAPTER 3: PEPTIDE AMPHIPHILE BASED HYDROGEL

Peptide amphiphile (PA) is a class of molecules composed of a hydrophobic tail and a hydrophilic head, in which the hydrophilic head is a peptide [21]

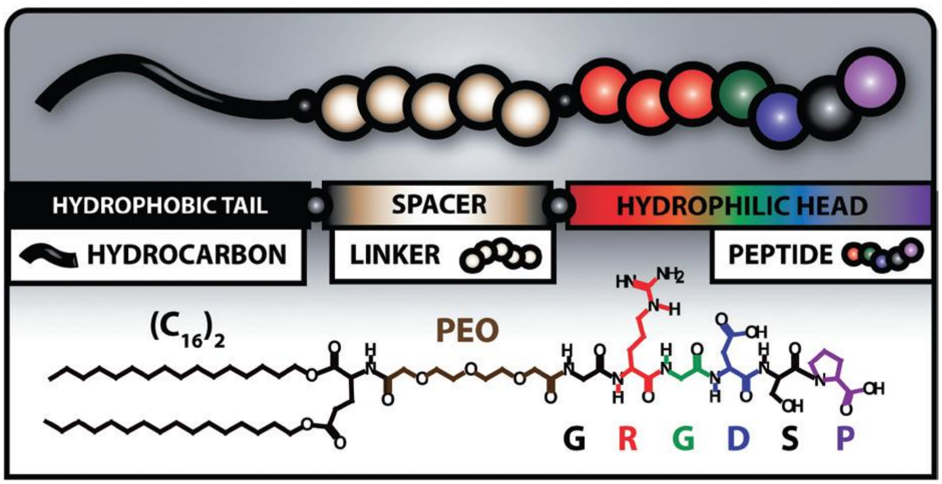

Figure 1. Structure of Peptide Amphiphile

"Adapted from reference Won H. Suh et, al. Polymer Adhesion, Friction, and Lubrication 2013. 283-316."

PAs can self-assemble into micelles or vesicles when in an aqueous environment. For instance, a hydrophilic head group will be exposed to the outside towards the water molecules and can form random coil, α-helix or β-sheet (like) structures, while a single-tailed hydrophobic lipid will induce the PAs to cooperatively assemble (self-assemble) and form micelles. Further, a PA hydrogel can form via additional hydrogen bonding, covalent tethering and/or the modulation of electrostatic interactions [22]. Many novel

PA hydrogels were developed in the past several decades. One recent PA hydrogel is a pH-responsive branched peptide amphiphile hydrogel called C_{16}-GSH (H_2N--SSSGGK(C16)HHH-C(O)-NH_2) [23]. The particular C_{16}-GSH peptide amphiphile that was studies for this thesis was H_2N-FAM-SSSGGK(C16)HHH-C(O)-NH_2 (Figure 2).

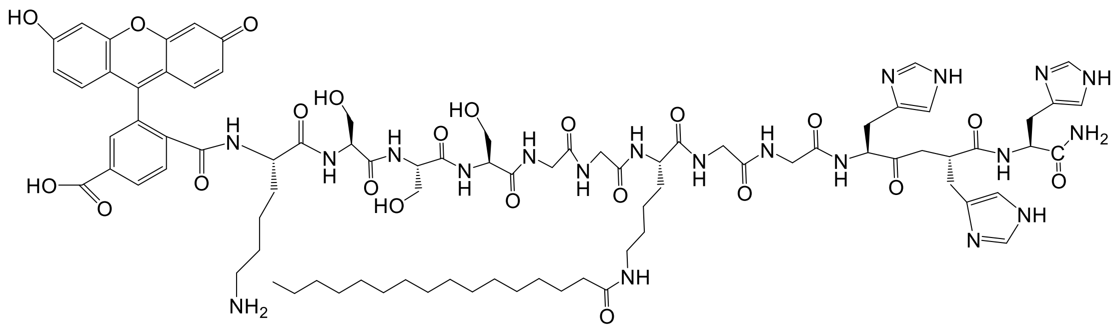

Figure 2. Structure of C_{16}-GSH

According to the article, the C_{16}-GSH can transform between the hydrogel state and the liquid state while in different pH ranges. In such a system, histidine plays a role as a key molecular switcher. The histidine has a pKa of approx. 6 [24]. When pH of the solution is above 7, about 90 % side chain imidazoles of histidine are in their basic form, and hydrogen bonds can formed between the side chains of histidine and serine. Basically, the hydrogel will be cross-linked by the hydrogen bonds. When the pH of solution is below 6, the histidine will be predominately protonated and become positive charged, resulting in the breakage of hydrogen bonds. Adjust the pH via NaOH will result in the formation of C_{16}-GSH hydrogels.

PA hydrogels are attractive as modular and synthetic extracellular matrices that can serve, in addition, as peptide-based drug delivery systems when coupled with bioactive PA molecules. The bioactive PA molecules can automatically mixed into the PA hydrogel system and incorporate into the micellar structures. Based on Tirrell and co-worker's recent research [25], PA micelles are expected to fall apart and become monomers again when in contact with cells and other macromolecules such as proteins. The individual PA monomers are, then, able to enter into mammalian cells. If such a scenario is to occur, our concern is that any of the PA monomers forming the hydrogel can potentially penetrate the cell membrane and get internalized since they all have hydrophobic tails. In order to confirm the hypothesis, cell internalization experiment of C_{16}-GSH (which is the structural component in the C16-GSH-based PA hydrogel) was conducted. C_{16}-GSH was synthesized via solid phase peptide synthesis (SPPS) and characterized via mass-spectrometry. For ease of observation, C_{16}-GSH was conjugated with FAM, a green fluorescence dye.

Peptide Amphiphile Synthesis

All peptide amphiphiles (C_{16}-GSH, SA1, and SA2) mentioned above were synthesized via solid phase peptide synthesis (SPPS). The SPPS was using porous beads (i.e., Rink Amid AM resin) with Fmoc-protected amine functional groups. The specific amino acids were conjugated to the Rink Amide AM resin one by one after Fmoc deprotection. The Fmoc deprotection solution was prepared with 20 % 4-methylpiperidine and 20 % DBU in 20 mL dimethylformamide (DMF). The peptides were shaken in the deprotection solution for 20 mins. The deprotection step was repeated 3 times. To conjugate the amino acids, conjugation solution consisting of 6 equiv. DIEA, 3 equiv. HOBT, and 3 equiv. HBTU in DMF solution was mixed with a specific (protected) amino acid and then shaken in the hood for at least 4 hours after the deprotection step. Fmoc-lysine(Dde)-OH was employed as a linker to conjugate with either acetic acid, palmitic acid and/or a fluorescence dye. Dde was removed with a solution of 200 µL hydrazine in 10 mL DMF. The bead-prepared PA molecules were cleaved from the resin using a cleavage solution composed of triisopropylsilane (TIS): water: TFA in a ratio of 2.5 %: 2.5 %: 95 % via treating for 4 hours. The crude PAs were precipitated in 20 mL of cold diethyl ether for 20 mins (3 times) and purified using reversed phase-high performance liquid chromatography (RP-HPLC). The purified PAs were dried in the lyophilizer, and exposed to the UV light 30 mins for sterilization. The sterilized PAs were dissolved in the filtered nano-pure water and prepared into 100 µM stock solutions.

Mass Spectrometry Result of C_{16}-GSH

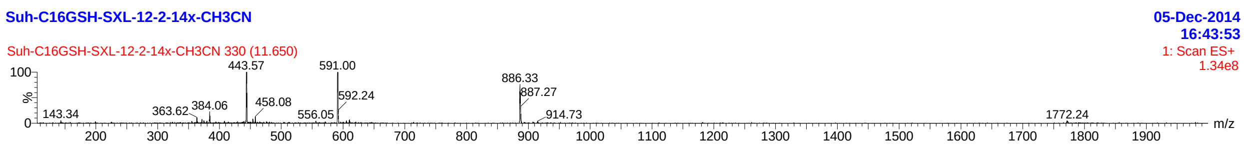

Figure 3. The mass-spectrometry result of C_{16}-GSH

Mass spectrometry results were obtained via a fee-based service offered at the Fox Chase Cancer Center to verify the molecular weight, synthesized. The expected molecular weight of C_{16}-GSH is 1769.98. The observed mass of C_{16}-GSH is 1772.24. Based on the result, we believe the sample synthesized via SPPS is H_2N-FAM-SSSGGK(C16)HHH-C(O)-NH_2 as shown in Figure 2.

Cell Internalization of C_{16}-GSH

For cell uptake experiments, A549 lung cancer cells were used as target cells. The cell number was 10,000 cell/well in an 8 well chamber slide. Three concentrations of C_{16}-

GSH (0.1 µM, 1 µM and 5 µM) were selected and treated for approx. 3 hours. After the 3 hour treatment, cells were rinsed with fresh medium 3 times for 10 mins to remove the extra C_{16}-GSH and subjected to live-cell imaging to verify cellular uptake. The results are provided in Figure 4 and they were obtained via fluorescence microscopy (Olympus IX-83) equipped with a live-cell stage-top incubator (LCI Chamlide).

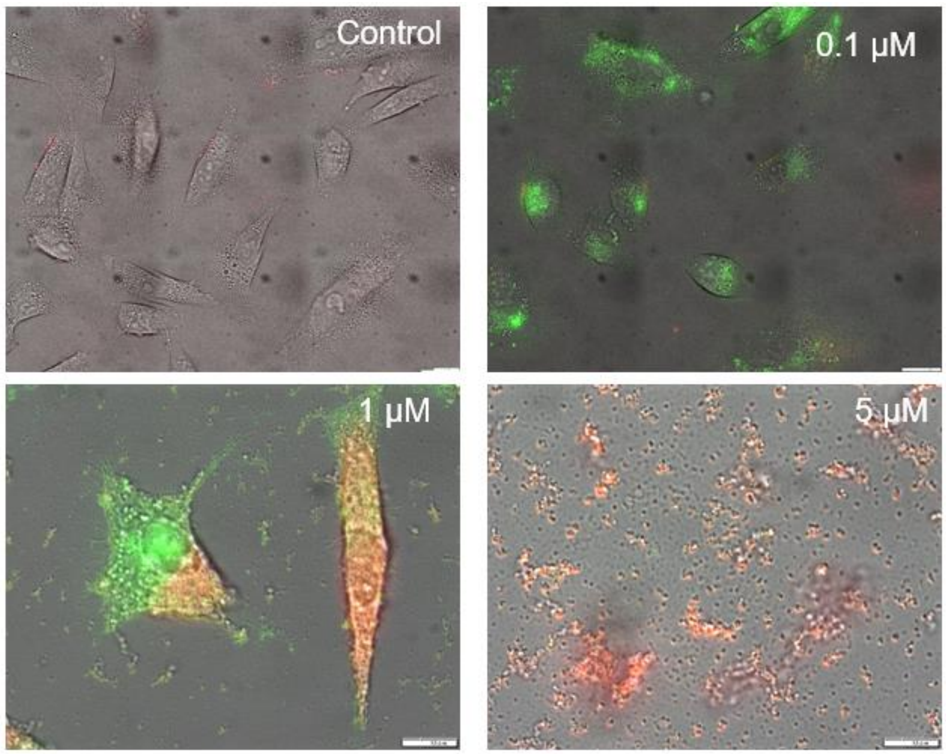

Figure 4. Cell Internalization of C_{16}-GSH Molecules. A549 cells were treated with 0, 0.1, 1 and 5 µM of PA for 3 hours. Scale bar: 20 µm.

In Figure 4, the green signal comes from the C_{16}-GSH.The results reveal that C_{16}-GSH molecules are capable of entering A549 cells in 2D cell culture conditions. The cell uptake efficiency of C_{16}-GSH is in a concentration-dependent manner. With the increasing concentration of C_{16}-GSH, the cell internalization efficiency increased. In addition, the cytotoxicity of C_{16}-GSH to the A549 cells were significant beginning from 1 μM concentrations. Apparently, high uptake of C_{16}-GSH (1 and 5 μM) into cells led to the death (and destruction) of A549 cells. In the Figure 4, some red fluorescent signals were detected. We assume these red signals are from auto fluorescence, as they also can be observed in the control group.

To sum up, the C_{16}-GSH, which has the capability to become hydrogels, can internalize into mammalian cells and, in certain concentration, induce cell death (1 and 5 μM). This internalization experiments prompted us that utilizing peptide amphiphile (PA) hydrogel systems for peptide or small molecular delivery work would not be a suitable choice moving forward. Under this premise, we chose to study alginate-based hydrogel systems as a new candidate for developing stem cell 3D culture systems (See Chapter 4).

CHAPTER 4: ALGINATE HYDROGEL

Alginate (or alginate acid) - a naturally derived polysaccharides isolated from brown algae - is widely used for tissue scaffold and drug delivery applications in bioengineering. One advantage of alginate is that the alginate is easily made and modified at relatively low costs. Alginate polymers are composed of (1-4)-linked β-D-mannuronic acid (M units) and α-L-guluronic acid (G units) monomers which vary in amount and sequential distribution along the polymer chain depending on the source of the alginic acid [26] (Figure 5).

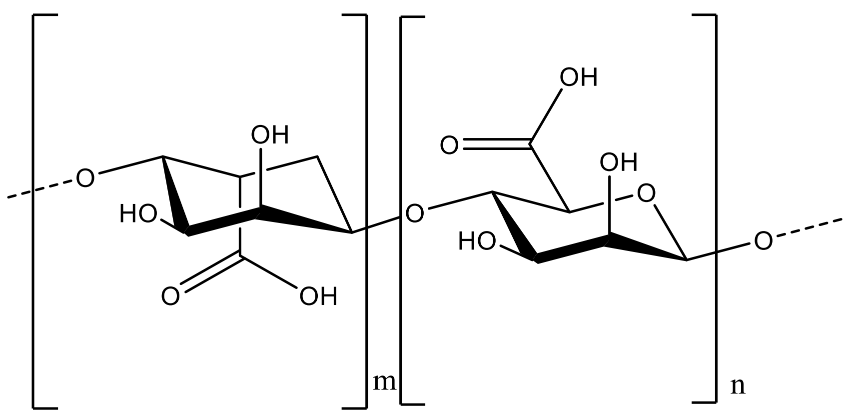

(G) Guluronic (M) Mannuronic

Figure 5. Chemical Structure of Alginate

The alginate molecule is a block copolymer composed of regions of M units, regions of G units and regions of tactically organized M and G units. Divalent cations such as calcium (Ca^{2+}) cooperatively cross-links the carboxylate groups in adjacent alginate chains together, creating ionic linkages that lead to the gelation of solubilized (sodium) alginate solutions [27].

Alginate exhibits several properties that enable it as the a potential matrix for various cell biology and drug delivery applications. First, it is biocompatible and biodegradable. The relatively mild gelation process allows soluble factors (including therapeutic agents) and living cells to be incorporated into the 3D matrix [28]. The porous structure of alginate hydrogels enable the diffusion of molecular drugs to the encapsulated cells. Furthermore, alginate hydrogels are very stable in the temperature range of 1~100 ℃. For instance, drug stability is retained even after freeze-drying occurs [29]. In addition, the mechanical property and the biological property of alginate hydrogels can be modified based on needs. The mechanical property of alginate hydrogel such as matrix stiffness and swelling rate can be controlled via modulating the cross-linking density or the molecular weight distribution [30]. The carboxylate groups on the alginate allow chemical modifications, in addition. One shortcoming of the alginate is that the cells cannot undergo specific cellular binding on the alginate surface because it has no cell-adhesive (or cell-binding) molecules. Conjugating RGD sequences to the carboxyl group via the formation of amide bonds [31], however, can lead to increased cell adhesion. In this thesis work experiment, the alginate was crosslinked in the $CaCl_2$ solution via ionic bond formations. By controlling the Ca^{2+} solution concentration, the alginate hydrogel's stiffness can be adjusted. Specifically, alginate hydrogels were prepared into having spherical shapes.

Alginate Bead Synthesis

The alginate solution was prepared in the concentration of 2 g/100 mL utilizing nanopure water and stirred for overnight at room temperature. The $CaCl_2$ solution was prepared in the concentration of 50 mM. The alginate and calcium chloride solution were all purified via 0.22 μm filtration processes. The purified alginate solution were mixed with a cell solution in the equal volumes and then pipetted into 50 mM $CaCl_2$ solution drop by drop to form alginate beads (spheres). Normally, 1 mL mixture solution can produce 20 alginate beads. After 2 mins, the extra $CaCl_2$ solution were removed and the alginate beads were rinsed 3 times with fresh medium for 10 mins, as excess $CaCl_2$ can be toxic to cells.

Cell Internalization of C_{16}-GSH in Alginate Hydrogels

In order to confirm whether the porosity of alginate hydrogels allows the penetration of small molecules, cell internalization experiment were conducted using C_{16}-GSH with alginate encapsulated cells (Figure 6). The incorporated cells in alginate beads were at 10,000 cells per bead density and they were incubated for 24 hours. After 24 hours of incubation, C_{16}-GSH of 1, 2, 5 μM were added into medium and incubated for another 24 hours. Old media were removed and the alginate hydrogels were rinsed with fresh medium for 10 mins to remove the excess C_{16}-GSH. Microscopy was performed via a Confocal Laser Scanning Microscope (LSCM) and a fluorescence microscope (Olympus IX-83) (Figure 6, 7).

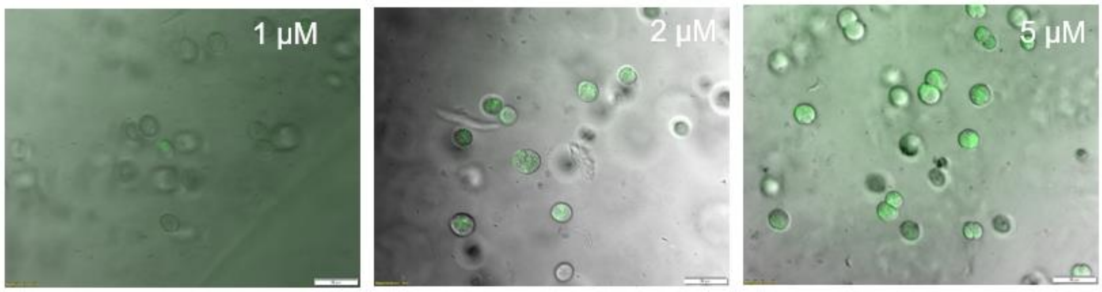

Figure 6. Live Cell Imaging of Alginate Encapsulated A549 Cells Treated with C_{16}-GSH (1 μM, 2 μM, 5 μM) (20X).

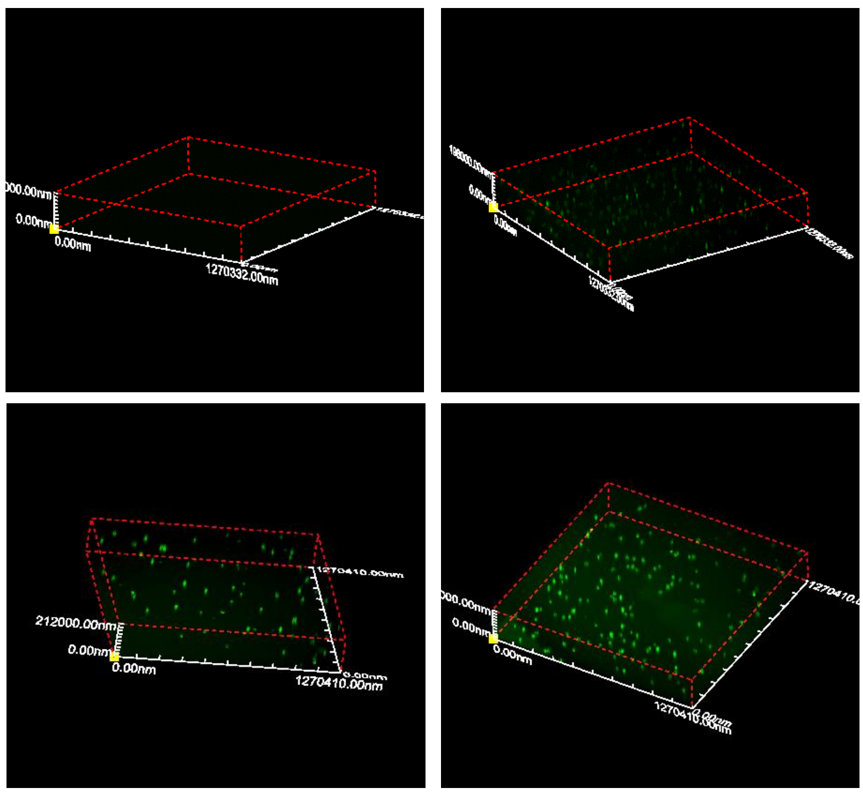

Figure 7. Cell Internalization of C_{16}-GSH of 0, 1, 2, and 5 μM in Alginate Hydrogels Analyzed via LSCM (10x).

Based on Figure 6 and Figure 7, cells were successfully encapsulated into the alginate hydrogel and was observed to be in healthy states after 48 hours incubation. The cells were in the globular (spherical) shape and the cell membrane were intact. Furthermore, C_{16}-GSH was observed inside the cells incorporated in the alginate hydrogels at all three concentrations. The penetration of C_{16}-GSH in the alginate beads showed same concentration-dependent manner as in the 2D culture system (Chapter 3). The difference was that the cells in the alginate bead were still alive even when the cells were treated with 5 μM C_{16}-GSH. This may be an matrix effect where the alginate structures interacted with the treated bioactive molecules (in this case, C_{16}-GSH). Basically, the polymeric components worked as a barrier slowing down the process of C_{16}-GSH interacting with the living cells. Compared to the 2D culture system (Figure 4), decreased C_{16}-GSH signals were observed at the same concentration (1 μM). This work leads us to believe that the 3D structure and porosity of the calcium alginate hydrogel can attenuate the penetration of molecules. In summary, this chapter's polysaccharide hydrogel experiments suggest that alginate's porous structures can modulate the penetration of peptide amphiphile molecules. Unfortunately, however, even with the favorable properties of calcium alginate hydrogels as mentioned and shown above as a 3D culture system, we encountered some technical difficulties when performing RT-qPCR experiments for the encapsulated cells in alginate hydrogels since no C_T values were obtained on multiple occasions. The reason, at the time of the experiments, were not so clear so we moved onto a photopolymeric system (Chapter 5).

CHAPTER 5: HYALURONIC ACID HYDROGEL

Hyaluronic acid (HA), a linear polysaccharide, is ubiquitous in the human body being present in the cartilage and nerve tissues. HA is an essential component in the extracellular matrix (ECM) of the brain, for instance, since it plays various critical role in modulating the cellular processes including cell proliferation, nerve regeneration, migration and neuronal development [32]. Pure and high molecular weight HAs can now be mass produced from bacterial cultures, which has no protein impurities compared to the HA from living tissue sources. Furthermore, HA can be degraded naturally by hyaluronidase in the body. The degradation rate can be determined by the molecular weight, degree of modification and crosslinking [33].

HA is one of the well-recognized and well-utilized biomaterial in tissue and stem cell engineering not to mention drug delivery applications. The HA polymer is composed of alternating units of *D*-glucuronic acid and *N*-acetyl-*D*–glucosamine (Figure 8).

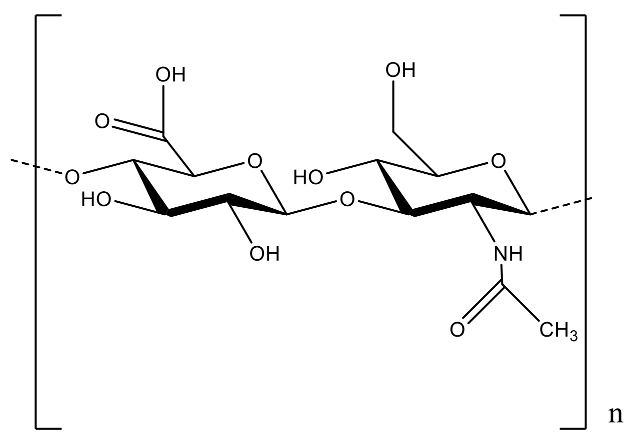

Figure 8. Chemical structure of Hyaluronic Acid

The HA contains several side functional groups that include the carboxyl group, the primary and secondary hydroxyl groups and the *N*-acetyl group that allows for tailored chemical modifications. The HA hydrogel system, for instance, can be cross-linked through various crosslinkers, such as adipic acid dihydrazide, maleimides or photo-reactive methacrylic anhydride [34].

Methacrylate group modification is the most common polymerizable reactive group tethering used in biomedical applications since it can undergo rapid crosslinking chemistries with the formation of radical initiators. One method for crosslinking HA hydrogel is using methacrylic anhydride to form methacrylated HA (MeHA) under basic conditions (pH>8) as shown in Figure 9 [35]. The basic environment is used to neutralize the formation of methacrylic acid, which can affect the solubility of HA polymers.

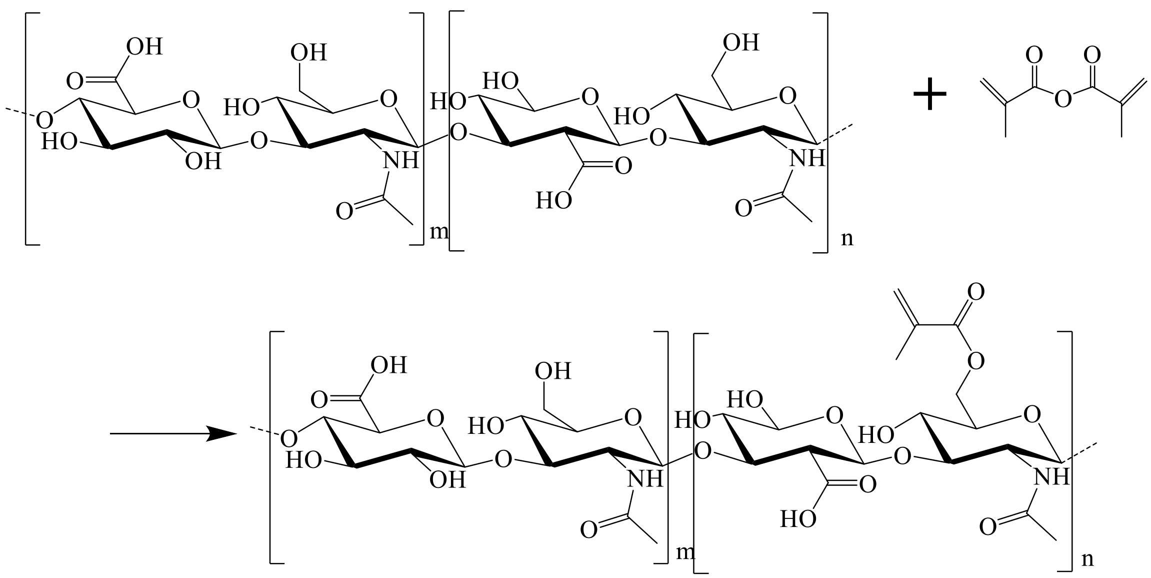

Figure 9. Reaction of Hyaluronic Acid with Methacrylic Anhydride

One advantage of utilizing MeHA is that the mechanical properties of the formed hydrogels can be adjusted by controlling the HA molecular weights and the number of reactive (methacrylate) groups. The utilization of 3D MeHA systems have been shown in neural stem cells differentiation research. For example, according to Schmidt and co-worker’s report, HA hydrogel systems that more closely recapitulate the mechanical properties of the neonatal brain would induce more neural progenitor cells (NPC) to become more neurons. In contrast, the same NPCs differentiated into more astrocytes than neurons when cultures within HA hydrogels that had mechanical properties identical to those of the adult brain [35]. For this thesis work, the mechanical properties of the MeHA hydrogels will be precisely controlled by adjusting the ratio of methacrylic anhydride to the HA and the light exposing time in order to induce the neural stem cell differentiation into neurons. The mentioned work is an adaptation of Weili Ma's MS thesis work from the Suh group at Temple University. According to his work, 5 molar excess of methacrylic anhydride can produce MeHA hydrogel with stiffness similar to the brain’s modulus. The adult human brain tissue which has been reported to be 2.7 kPa and 3.1 kPa for white and grey matter, respectively [36]. The MeHA hydrogel will be ultimately cross-linked via radical polymerization. A photo-initiator was used to produce the free radical to induce the radical polymerization of MeHA molecules. An intense metal-halide light source (e.g., over 1 W/cm^2) was utilized to activate the free radicals that incorporated UV light wavelength ranges (250-400 nm).

Hyaluronic Acid Hydrogel Preparation

MeHA solution was prepared by the addition of methacrylic anhydride (Alfa Aesar) to a solution of HA (Lifecore, MW=1100 kDa). HA powders were dissolved in nanopure water in the concentration of 10 mg/m, first. The dissolved HA solution was then mixed with methacrylic anhydride in the ratio of 5:1 at 4 ℃ conditions. The pH should be adjusted above 8.0 through the reaction conditions. When the pH is below 8.0, 5 M NaOH should be added drop-by-drop to increase the pH. The reaction duration was kept at 24 hours in the refrigerator. Dialysis was conducted to remove the extra impurities in the MeHA solution such as excess NaOH. The dialysis step took about 2~3 days after the esterification reaction step. The water was changed every day. The final product was obtained by lyophilization. The lyophilized MeHA were rehydrated in the photo initiator (Irgacure 2959) included solution (0.05 % wt. /vol). The rehydrated MeHA solution then was transferred into the 48 well plate. Each well was filled with 100 μL MeHA solution. The MeHA solution in the wells was exposed to an intense bright light (Light source: EXFO X-CITE 120Q) for 10 seconds to initiate the radical polymerization process. The cross-linked MeHA hydrogels were lyophilized again, overnight, to increase the porosity. The lyophilized MeHA hydrogel was then transferred to a new 24 well plate and exposed to cell culture hood UV light for 30 mins (both sides) for sterilization purposes. The MeHA hydrogel was rehydrated via adding 200 μL of cell medium (re-wetting process take approx. 20 mins). After 20 mins of swelling, another 200 μL fresh medium was added.

Cytotoxicity Assay of Bioactive Molecules

WST-8 (Dojindo, Inc.) was utilized to measure the cytotoxicity of DHED, compound B and LiCl. The cell type was ReNCell VM (RVM; Millipore, Inc.). SA1 and SA2 toxicities were figured out by another researcher in the Suh Lab and the developed protocol was utilized. Briefly, RVMs were seeded into 96 well plates at a density of 9,000 cells/well in 100 μL medium and incubated for 24 hours. Bioactive molecules of different concentrations were added into the 96 well plates and incubated for another 24 hours. 10 μL WST-8 solution was added into each well and incubated for 1 hour. Absorbance at 450nm were measured by using a microplate reader (Tecan Infinite 200 Pro). Each samples were prepared in triplicates. DHED was dissolved in DMSO at the density of 10 mM first, and then diluted in nanopure (sterile) water. Compound B and LiCl were dissolved in the nanopure water.

Cell Differentiation Experiment of hNSCs

For 2D cell culture systems, 24 well plates were coated with 20 % laminin in DMEM/F12 medium for 4 hours before cell seeding. Neural stem cells were seeded into 24 wells at the density of 80,000 cell/well after the laminin coating process. For 3D culture systems, cell number in each well was 200,000 cell/well. 200 μL cell solution were added onto the MeHA hydrogel and incubated for 20 mins so that the cells are able to penetrate (incorporate) into the hydrogel. Another 200 μL media were added to the hydrogel after 20 mins. Epidermal growth factors (EGF) and basic fibroblast growth factor (bFGF) were included in the medium. To initiate the neural stem cell differentiation, the medium was changed to NSC maintenance medium without EGF and bFGF, but with the chosen bioactive molecules and ions (LiCl, DHED, Compound B, SA1, and SA2) dissolved. The cell media were changed every other day. The bioactive molecules were treated to the cells with medium every other day until day 7 and day 14 at which time RT-qPCR and ICC experiments were conducted.

Quantitative Reverse Transcript Polymerase Chain Reaction (RT-qPCR)

For 2D cell culture systems, the mRNAs were isolated and purified using an Ambion mirVana kit (life technologies). The concentration and purities of mRNAs were analyzed using a microplate reader (Tecan Infinite 200 Pro). For 3D cell culture systems, the cells were treated with the medium mixed with 100 U/mL hyaluronidase one day before collecting the cells. The HA hydrogels degraded overnight. The dissolved HA and cell solutions were collected and centrifuged for 5 mins at 500 rcf to collect the cell pellets. The mRNAs were collected using an Ambion mirVana kit (life technologies). The detailed procedures of mRNA collection， cDNA synthesis and RT-qPCR are shown below:

mRNA collection

1. Warm up elution solution to 60 degree Celsius.
2. Wash the cells with PBS once.
3. Remove PBS and add 300 μL of lysis buffer.
4. Transfer to 1.5 mL centrifuge tube.

5. Add 30 μL homogenate solution.
6. Put in ice for 10 mins.
7. Add 330 μL of phenol-chloroform (in the chemical fume hood)
8. Vortex for 1 min.
9. Centrifuge at 7200 rcf for 7 mins at 4 degree Celsius
10. Collect aqueous layer in sterile 1.5 mL centrifuge tube and discard phenol-chloroform in appropriate container.
11. Add 495 μL of ethanol to collection tube.
12. Vortex for 30 sec.
13. Transfer to special RNA filter tube and centrifuge at 7200 rcf for 30 sec at 4 degree Celsius.
14. Remove ethanol solution and wash the filter with 700 μL of washing solution 1 and centrifuge with same setting.
15. Remove washing solution and wash filter twice with 500 μL of washing solution 2/3 and centrifuge with same setting.
16. Remove washing solution and add 100 μL of elution solution and centrifuge with same setting.
17. Take reading with nanoquant plate:
18. Requirement: concentration >60 ng/μL

    OD260/280: 1.9~2.1

cDNA Synthesis

1. Dilute all mRNA to the same concentration using Nuclease free water in the new cDNA synthesis tube. The total mRNA volume should be 10 mL.

2: Mix all the chemical listed together:

- mRNA: 10 μL
- RT buffer: 2 μL
- 25X dNTP master: 0.8 μL
- 10X RT random primer: 2 μL
- Multiscribe reverse transcriptase: 1 μL
- Nuclease free water: 4.2 μL

Total volume: 20 μL

3. Centrifuge the tube to make sure all the solution are on the bottom.

4. Run the cDNA program in PCR machine.

RT-qPCR

After cDNA synthesis, mix 1.1 μL cDNA with the chemical listed below in the MicroAmp Fast 96-Well Reaction Plate (applied Biosystems):

- cDNA: 1.1 μL
- Master mix: 5 μL
- Primer mix: 0.5 μL
- Water: 3.5 μL

Total Volume: 10.1 μL

Primer choices: Nestin, Sox2, MAP2, Tubb3, GFAP, OMG, β-actin, GAPDH.

Nestin, Sox 2: Neural stem cell marker

MAP2, Tubb 3: Neuron marker

GFAP: Astrocyte marker

OMG: Oligodendrocyte marker

B-actin, GAPDH: House keep genes

1. Cover the 96 well plates to prevent the degradation and evaporation.
2. Mix all the solution using centrifuge to remove any bubbles in the wells. The bubble can influence the read of FAM density.
3. Run the RT-qPCR program, collect the CT value after the program is finished. The CT value should not be over 40.

Immunocytochemistry (ICC)

1. The differentiated cells were fixed with 4% paraformaldehyde for 10 mins at room temperature, and then washed with cold PBS for 3 times.
2. Permeabilize the cells with Blocking solution (0.3% Triton®-X and 3% Donkey serum solution (diluted in the PBS) for 30~60 minutes at room temperature.
3. Remove the blocking solution, and coat the cells with primary antibody diluted in the blocking solution (ratio 1:200).
4. Incubate the coated cells at 2–8 ℃ overnight.
5. Wash the cells with PBS three times.
6. Coat the cells with second antibody diluted in the PBS (ratio 1:200) away from light for 1 hours.
7. Remove the solution and wash the cells with PBS 3 times for 10 mins away from light.
8. Add diluted DAPI solution for 15 mins away from light, and then wash the cells with PBS 3 times for 10 mins
9. IX-83 fluorescence microscope was used to capture the image.

CHAPTER 6: RESULTS AND DISCUSSIONS

Results of Cytotoxicity Assays

In order to test the cytotoxicity of the bioactive molecules (LiCl, DHED, and compound B), WST-8 assays were performed. According to the cytotoxicity assay results, DHED of 2 μM, LiCl of 3 mM, and compound B of 0.01 mg/mL concentrations were selected for performing long–term RVM differentiation experiments. As for SA1 and SA2, 0.1 μM will be utilized based on previous experiments within the Suh Lab.

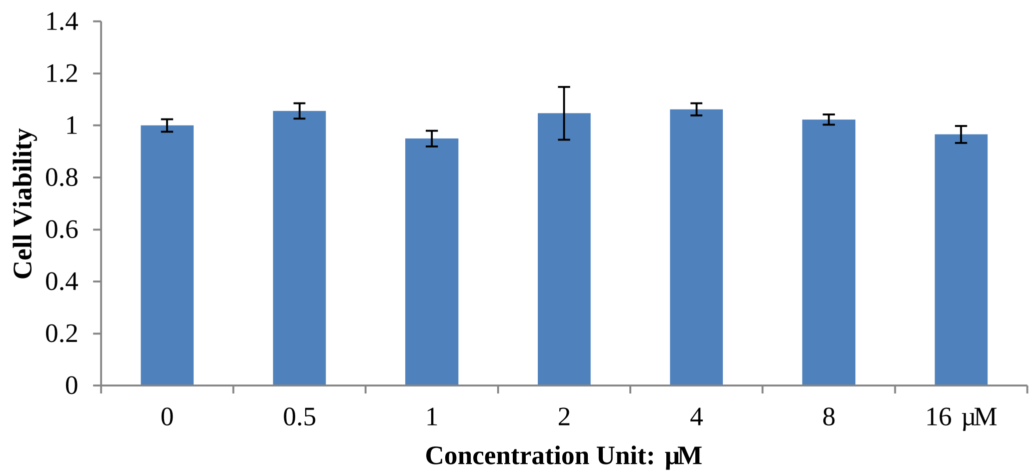

Figure 10. DHED RVM Cytotoxicity after 24 Hour Treatment (N = 3)

The result (Figure 10) showed that even at 16 μM, the viability of DHED treated cells were as high as 99 % compared to the control group after 24 hours. But when the concentration jumped to the 100 μM in the pure DMSO, the toxicity increased rapidly (result not shown).

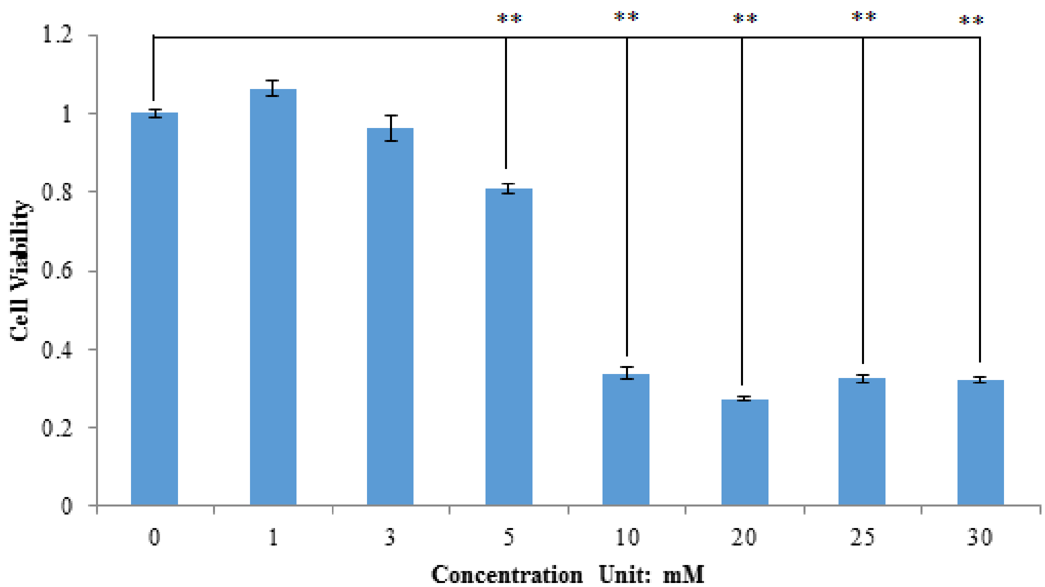

Figure 11. LiCl RVM Cytotoxicity after 24 Hour Treatment (**p<0.01, N = 3)

The result (Figure 11) presented that the cytotoxicity increased with the concentration of LiCl went higher. The cytotoxicity remained at a low level when the LiCl's concentration was below 5 mM. The viability was around 95 % when the LiCl concentration was 3 mM.

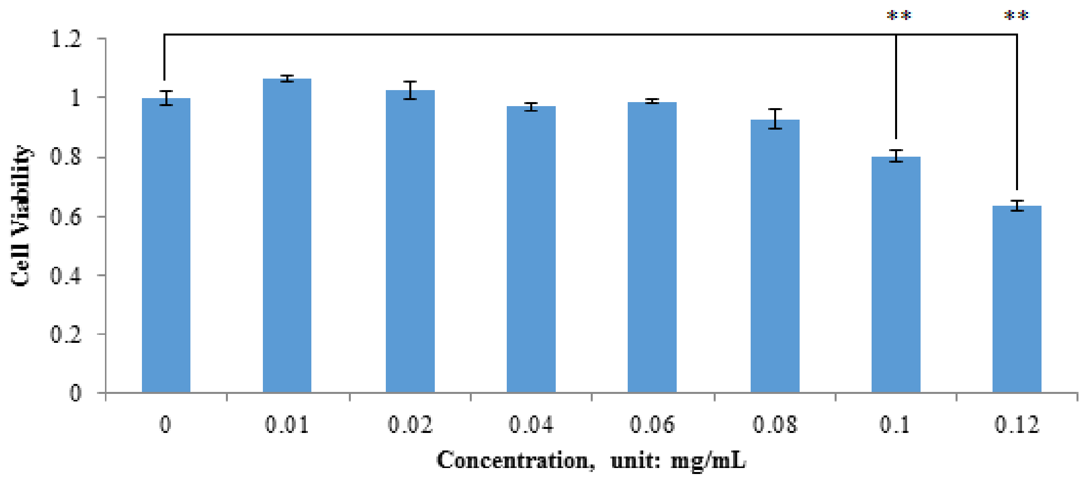

Figure 12. Compound B RVM Cytotoxicity after 24 Hour Treatment (**p<0.01, N = 3).

The compound B was very toxic to the RVM. In the first trial, compound B concentration from 0.25 mg/mL to 1 mg/mL were tried. The viability dropped to 50 % after 24 hours. When the concentration of compound B decreased to 0.01 to 0.12 mg/mL, the viability highly increased (Figure 12). The concentration below 0.08 mg/mL is safe to the RVM.

Microscopy Analysis of RVM in the 2D Cell Culture System

Image of the cell differentiation in 2D culture system treated with bioactive molecules from day 1 – day 14.

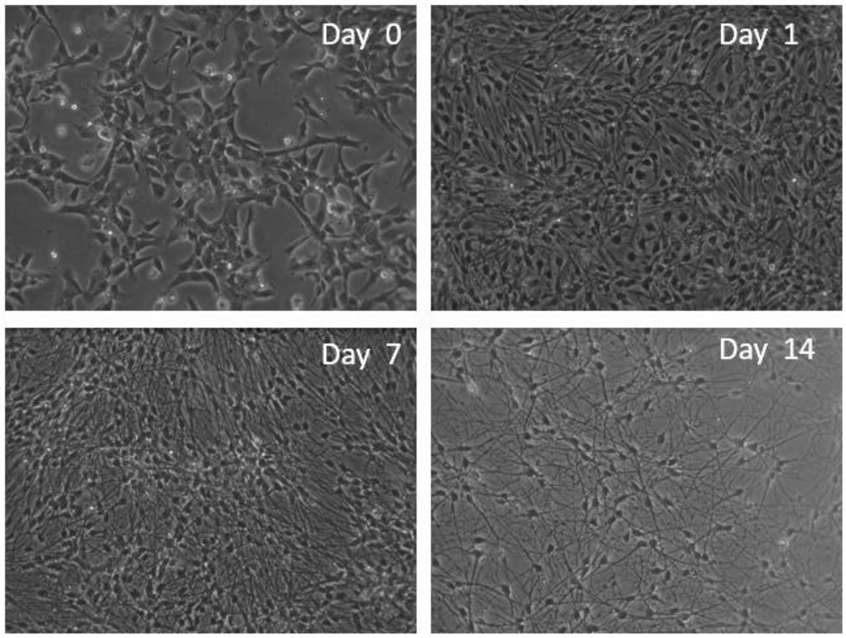

Figure 13. The differentiation image of RVM, no treatment control (day 0, 1, 7 and 14).

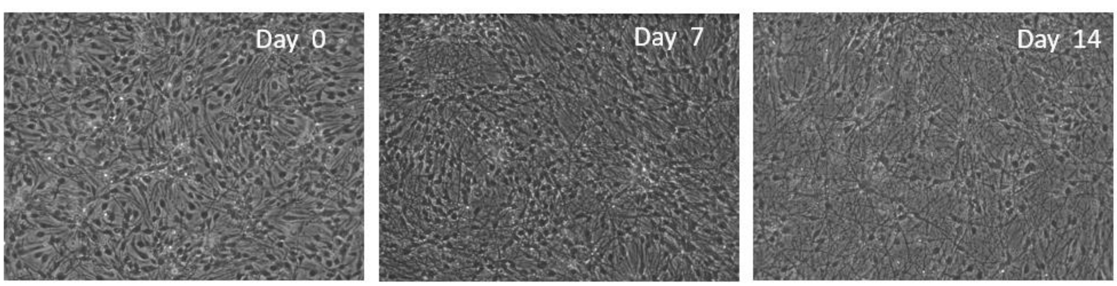

Figure 14. The differentiation image of 3 mM LiCl treated RVM (day 1, 7 and 14).

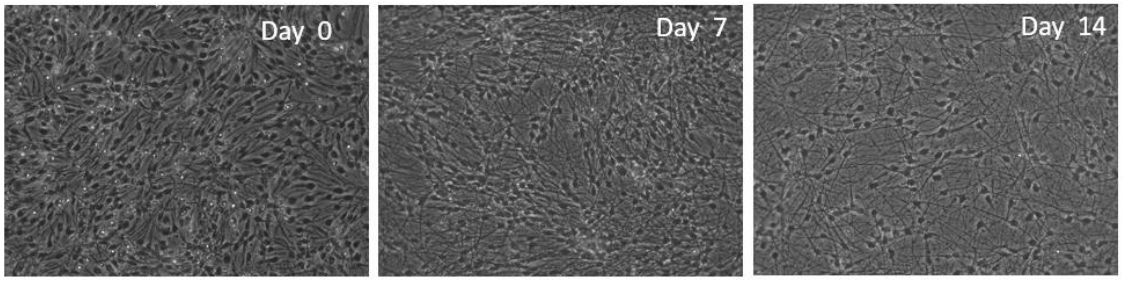

Figure 15. The differentiation image of 2 μM DHED treated RVM (day 1, 7 and 14).

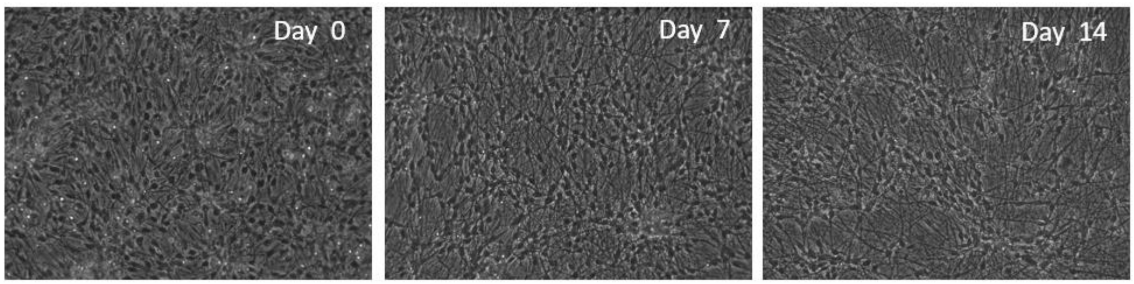

Figure 16. The differentiation of 0.1 μM C_{16}-pepB treated RVM (day 1, 7 and 14).

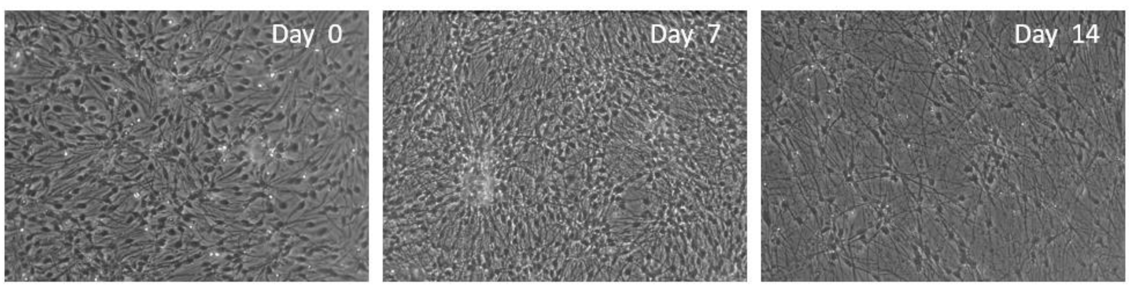

Figure 17. The differentiation image of 0.1 μM RA-Pep treated RVM (day 1, 7 and 14).

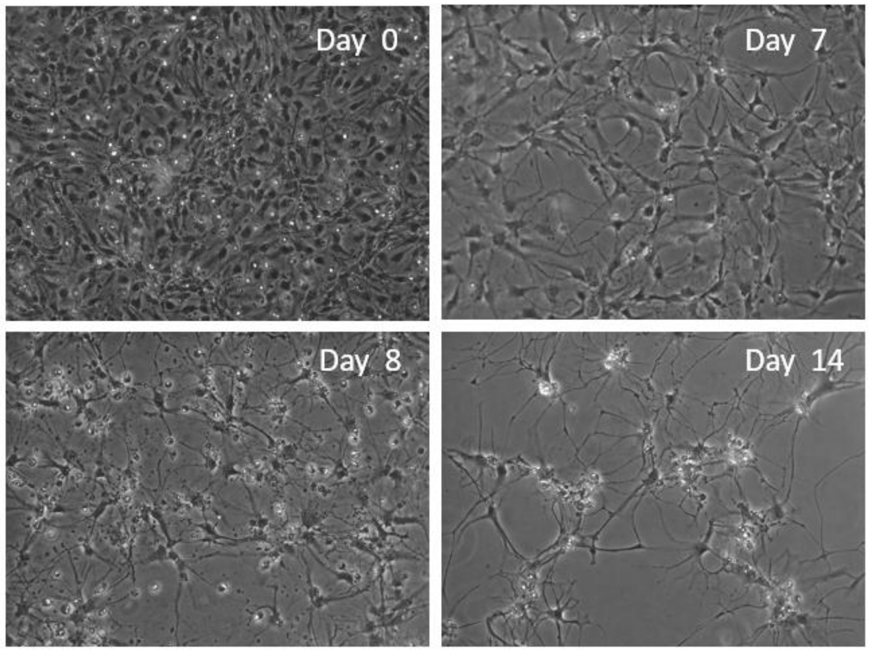

Figure 18. The differentiation image of 0.01mg/mL Compound B treated RVM (day 1, 6, 7 and 14).

After 14 days of differentiation, cells treated with LiCl, DHED, SA1, and SA2 differentiated normally and in healthy-looking conditions compared to the no treatment control (Figure 13-17). As for compound B treated cells, RVM cell numbers decreased rapidly after 7 days of differentiation. From day 7 through day 14, cell numbers continued to drop. On day 14, only 20 % of the initial cells can be observed via optical microscopy analysis (Figure 18). It is suggested that compound B may has a chronic cytotoxic effect on differentiation RVM cells.

Immunocytochemistry Analysis for the 2D Culture System

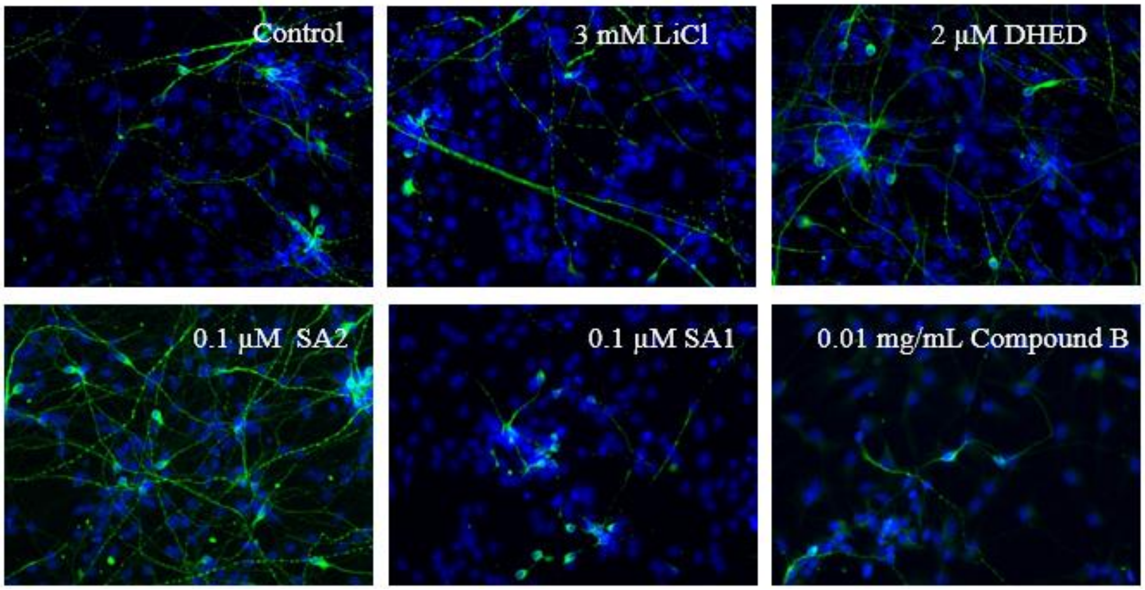

Figure 19. 1 week differentiation of DHED, LiCl, SA1, SA2, and Compound B (from top to the bot, and left to the right) treated RVM in 2D cell culture system. DAPI: Blue, Tubb-3: Green.

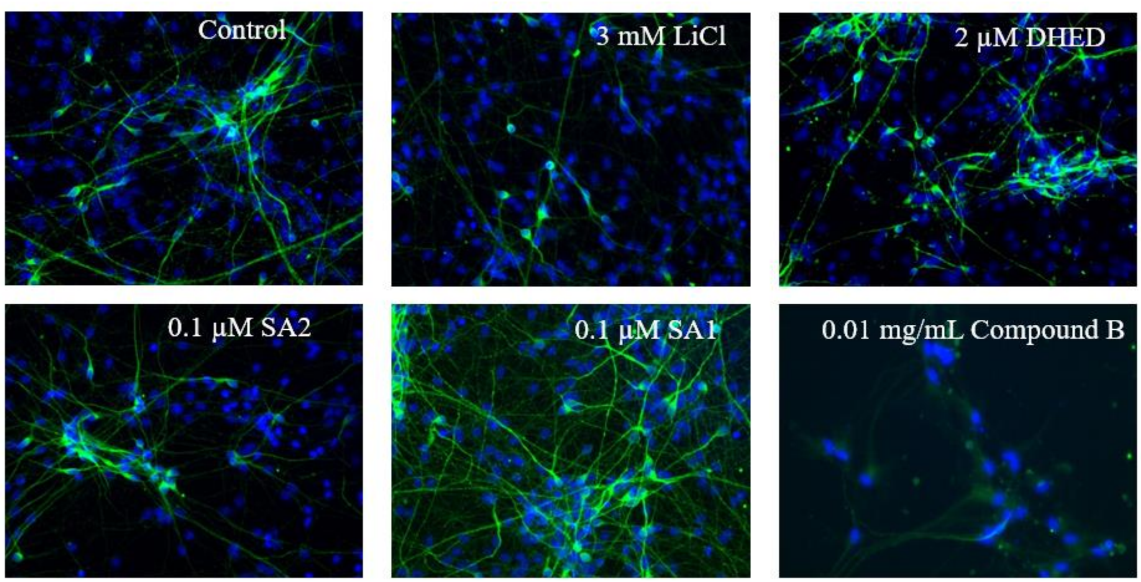

Figure 20. 2 week differentiation of control, DHED, LiCl, SA1, SA2, and Compound B (from top to the bot, and left to the right) treated RVM in 2D cell culture system. DAPI: Blue, Tubb-3: Green.

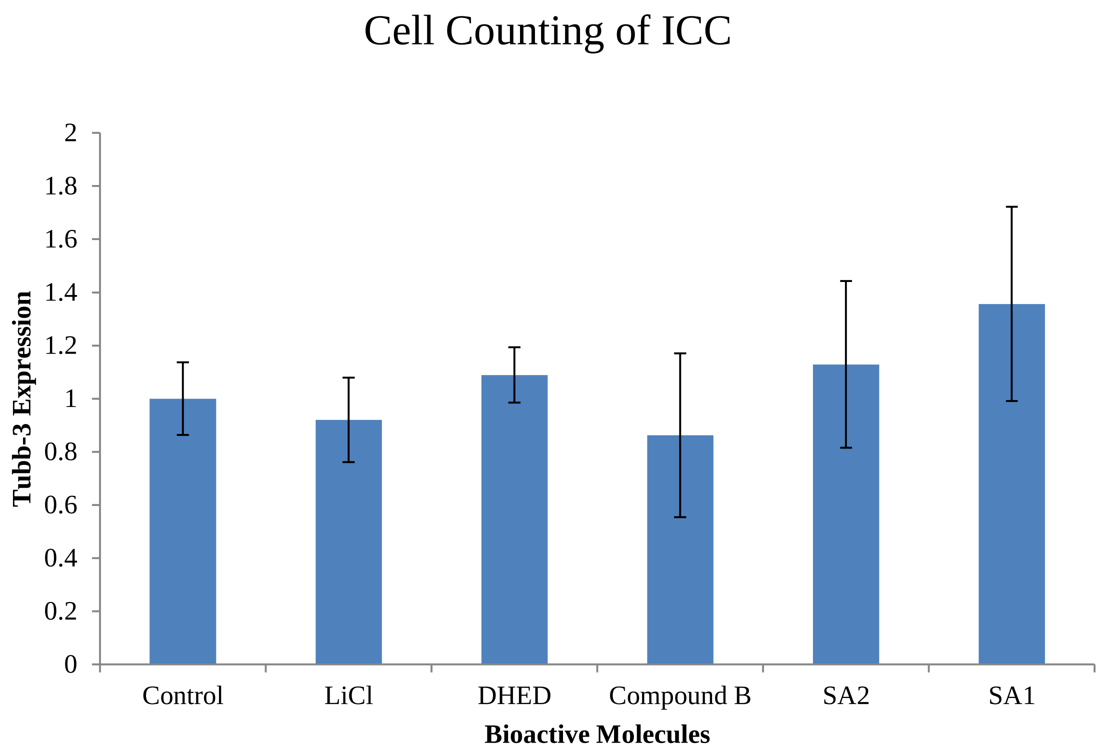

Figure 21. Quantification of cells expressing β3-tubulin (Tubb3) after 1 week differentiation in 2D culture system by cell counting. ICC microscopy images at 20x magnification (N=3).

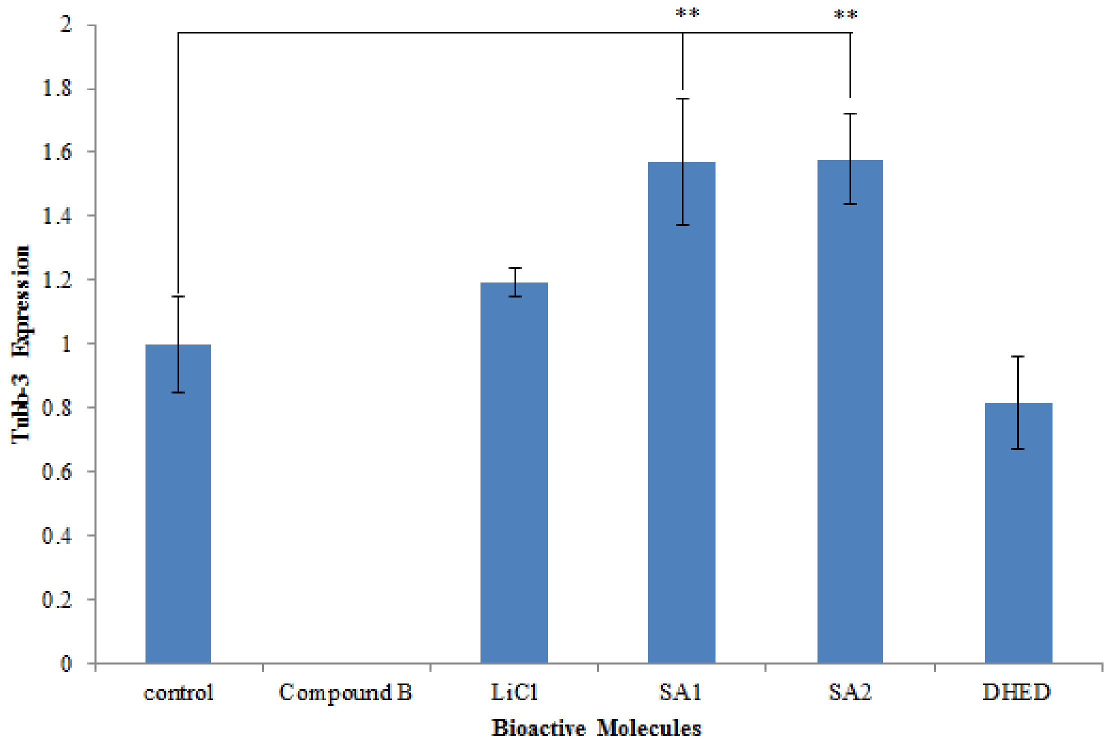

Figure 22. Quantification of cells expressing β3-tubulin (Tubb3) after 2 week differentiation in 2D culture system by cell counting ICC microscopy images at 20x magnification (**$p<0.01$, N=3).

In the 2D culture system, Tubb3, which is a neuron marker, expression levels can be quantified for both week 1 and week 2 samples (Figure 19, 20). In the week 2 samples, more Tubb3 expression can be seen compared to the week 1 samples in all groups. According to the quantification result (Figure 21), no statistical significance was seen amongst week 1 samples. In week 2, however, SA1 and SA2 has significant more Tubb-3 expression levels (1.6 fold) compared to the control group (Figure 22).

2D RT-qPCR Results

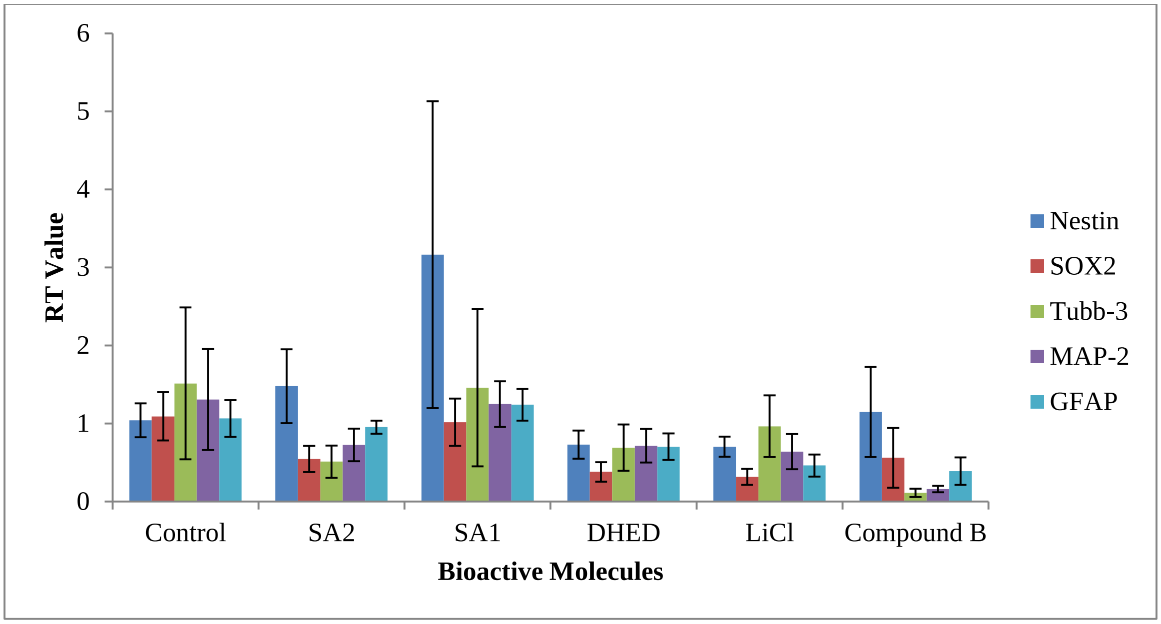

Figure 23. RT-qPCR result of 1 week differentiation in the 2D Culture System (N = 3).

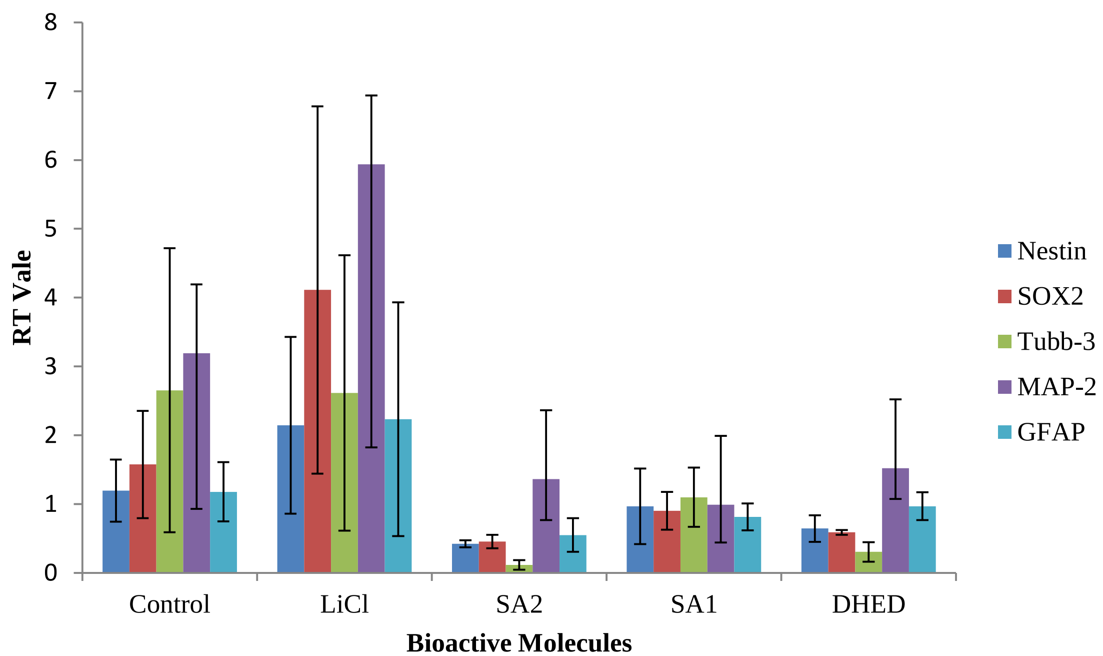

Figure 24. RT-qPCR result of 2 week differentiation in the 2D culture system (N=3).

RT-qPCR experiments were conducted to quantify the mRNA expression levels for the differentiated RVM cells. Nestin, Sox2, Tubb3, Map2 and GFAP were measured in the 2D samples. Based on the results (Figure 23, 24), no significance difference of mRNA expression levels of Tubb-3 were observed amongst all the groups for both week 1 and week 2 samples.

Microscopy Analysis of Cell Encapsulated in MeHA Hydrogels

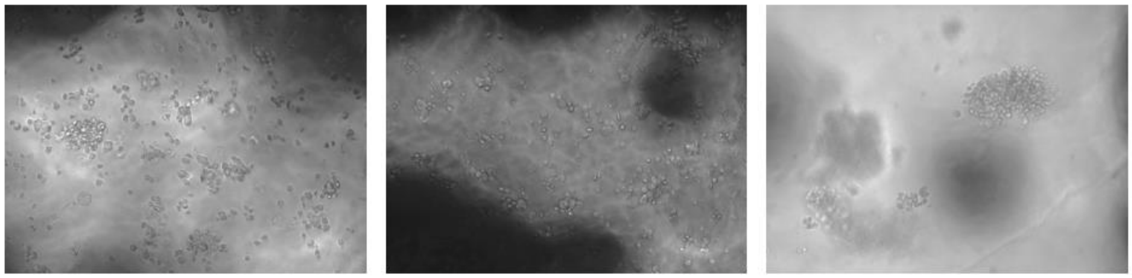

Figure 25. hNSCs encapsulated in the MeHA hydrogel for 24 hours.

The MeHA hydrogels have large swelling ratios. In our hypothesis, cells should be transferred into the hydrogel during the rehydration step of the hydrogel. But the results were not as expected. In the first two images in Figure 25, large quantities of cells can be observed on the surface of the 24 well plate and not inside the hydrogels. The hydrogel appears to be on top of the cells. It appears that most of the cells went to the bottom of the plates after the 24 hour incubation period instead of the RVM cells incorporating into pore of the MeHA hydrogels. Even though some cells can be observed inside the MeHA hydrogel (far right image in Figure 25), the cell density was lower compared to the cells outside the hydrogel. In the MeHA hydrogel, cells aggregated together to form clusters. After 7 days of incubation, no cell pellets were possible to collect after degrading the MeHA hydrogel using hyaluronidase. This was because large quantities of cells were lost during media changes during the 7 day differentiation period.

ICC in the MeHA for 1 Week Differentiation

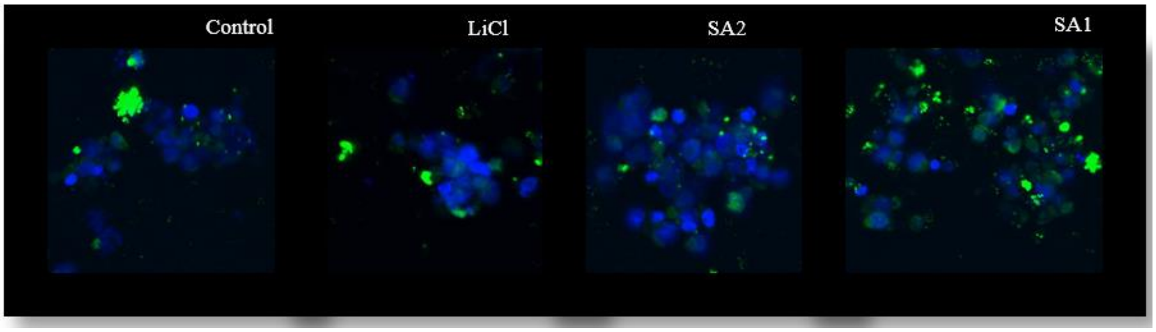

Figure 26. ICC Results (Control, LiCl, SA1, and SA2) of One Week RVM Differentiation in MeHA Hydrogels. (DAPI: Blue, Tubb-3: Green, 20X)

Nucleus was stained with DAPI. The Tubb-3 was stained with green. The images were captured using a laser scanning confocal microscope. While doing the ICC staining for 3D samples, exactly the same protocols were utilized as did in the 2D culture system. Most cells aggregated together in the MeHA hydrogel. According to the ICC result (Figure 26), no significant Tubb-3 expression was observed in the control, LiCl, and SA2 treatment groups. Multiple single cells were observed to have Tubb-3 green signals only in the SA1 treatment conditions.

CHAPTER 7: CONCLUSIONS AND FUTURE DIRECTIONS

Three hydrogel systems were investigated in this thesis work that include peptide amphiphiles (C_{16}-GSH), alginate and hyaluronate hydrogels. The cell internalization results of C_{16}-GSH tells us that both structural and bioactive peptide amphiphiles (lipidated peptide) can get internalized into the cells and potentially cause unknown biological effects. This means careful considerations will be to taken when utilizing peptide amphiphile (PA) hydrogels as 3D molecular and/or cellular delivery systems.

The alginate and methacrylated HA hydrogels were further developed for human neural stem cell (hNSC) work as an alternative to the PA hydrogel system and they were successfully synthesized and shown to have excellent biocompatibility for hNSC cell cultures. In the alginate hydrogel system, cells can be successfully encapsulated for long-term differentiation with high cellular densities but the RT-qPCR analysis issues hindered its further development. As for the MeHA hydrogel system, the main limitation is that after 1 week of differentiation, isolatable cell numbers were too low to get any significant amounts of mRNAs. The utilization of both ionic and photopolymerization methodologies may be the key to successfully developing 3D culture systems to eventually achieve hNSC differentiation to neurons.

Five bioactive molecules (LiCl, DHED, SA1, SA2, and compound B) were tested for neural stem cell differentiation and we established some baselines through this thesis work. Even though cytotoxicity was measured in advance and low concentrations were utilized during the differentiation experiment, the cell number of 0.01 mg/mL compound B treated cells decreased substantially after 2 weeks of differentiation. For future experiments, the concentration of compound B will need to be modulated further.

No significance difference of beta-3-tubulin protein expression levels was observed among the six 2D samples. In week 2 samples, more protein beta-3-tubulin proteins were expressed in all samples compared to the week 1 samples. SA1 and SA2 molecules, especially, increased the beta-3-tubulin expression levels approx. 1.6 fold compared to the control. Based on the ICC results, SA1 and SA2 showed positive effects on the neuronal differentiation after 2 weeks of differentiation. But when it comes to the RT-qPCR results, no significance differences were observed. As the mature differentiation of hNSCs to neurons takes at least 6 weeks for human cells, short-term (1 week and 2 week) expression levels of the analyzed proteins and their mRNA expression levels may be difficult to distinguish and clearly define. Furthermore, the stability of mRNA during the isolation processes may be an issue, at this current time [37]. Additional experiments will need to be conducted to be able to more precisely define the expression levels of Sox2, Nestin, Tubb-3, Map2, GFAP in one and two-week differentiated RVM cells.

In the MeHA hydrogel system, 1 week differentiation of hNSCs was conducted for ICC analysis. ICC results suggest that no beta-3 tubulin expression can be observed in the control group, LiCl, and SA2 groups. In the SA1 treated group, beta-3-tubulin can be clearly observed in some of the cells. More experiments (more cells) are again needed to conduct further RT-qPCR analysis.

In summary and based on the 2D ICC results, we believe that SA1 and SA2 are capable of increasing beta-3-tubulin expression in the protein level of hNSCs in 2D culture conditions after 2 weeks of differentiation. As for the 3D culture systems, the cell seeding protocol of MeHA should be optimized to increase the cell encapsulation rates and additional issues involving RT-qPCR will need to be addressed for the alginate system. Last but not least, in order to verify the effects of the chosen bioactive molecules and ions on the neuronal differentiation pathways, 4-week and 6-week differentiation experiments involving hNSCs will need to be conducted both for the 2D and 3D culture systems in the near future.

REFERENCES

[1] F. I. Tarazi, Z. T. Sahli, M. Wolny, and S. A. Mousa, "Emerging therapies for Parkinson's disease: From bench to bedside," *Pharmacology & Therapeutics,* vol. 144, pp. 123-133, Nov 2014.

[2] J. Jankovic and W. Poewe, "Therapies in Parkinson's disease," *Current Opinion in Neurology,* vol. 25, pp. 433-447, Aug 2012.

[3] O. Lindvall, Z. Kokaia, and A. Martinez-Serrano, "Stem cell therapy for human neurodegenerative disorders - how to make it work," *Nature Medicine,* vol. 10, pp. S42-S50, Jul 2004.

[4] B. Y. Hu, J. P. Weick, J. Y. Yu, L. X. Ma, X. Q. Zhang, J. A. Thomson*, et al.*, "Neural differentiation of human induced pluripotent stem cells follows developmental principles but with variable potency," *Proceedings of the National Academy of Sciences of the United States of America,* vol. 107, pp. 4335-4340, Mar 2010.

[5] J. E. Forde and T. C. Dale, "Glycogen synthase kinase 3: A key regulator of cellular fate," *Cellular and Molecular Life Sciences,* vol. 64, pp. 1930-1944, Aug 2007.

[6] C. Lange, E. Mix, J. Frahm, A. Glass, J. Muller, O. Schmitt*, et al.*, "Small molecule GSK-3 inhibitors increase neurogenesis of human neural progenitor cells," *Neuroscience Letters,* vol. 488, pp. 36-40, Jan 2011.

[7] H. F. Li, Q. Li, X. N. Du, Y. Y. Sun, X. Y. Wang, G. Kroemer*, et al.*, "Lithium-mediated long-term neuroprotection in neonatal rat hypoxia-ischemia is associated with antiinflammatory effects and enhanced proliferation and survival of neural stem/progenitor cells," *Journal of Cerebral Blood Flow and Metabolism,* vol. 31, pp. 2106-2115, Oct 2011.

[8] F. Takahashi-Yanaga, "Activator or inhibitor? GSK-3 as a new drug target," *Biochemical Pharmacology,* vol. 86, pp. 191-199, Jul 2013.

[9] G. Castelo-Branco, N. Rawal, and E. Arenas, "GSK-3 beta inhibition/beta-catenin stabilization in ventral midbrain precursors increases differentiation into dopamine neurons," *Journal of Cell Science,* vol. 117, pp. 5731-5737, Nov 2004.

[10] A. K. Silva, H. Yi, S. H. Hayes, G. M. Seigel, and A. S. Hackam, "Lithium chloride regulates the proliferation of stem-like cells in retinoblastoma cell lines: a potential role for the canonical Wnt signaling pathway," *Molecular Vision,* vol. 16, pp. 36-45, Jan 2010.

[11] C. Jamieson, M. Sharma, and B. R. Henderson, "Regulation of beta-Catenin Nuclear Dynamics by GSK-3 beta Involves a LEF-1 Positive Feedback Loop," *Traffic*, vol. 12, pp. 983-999, Aug 2011.

[12] B. T. Tan, L. Wang, S. Li, Z. Y. Long, Y. M. Wu, and Y. Liu, "Retinoic acid induced the differentiation of neural stem cells from embryonic spinal cord into functional neurons in vitro," *International Journal of Clinical and Experimental Pathology,* vol. 8, pp. 8129-8135, 2015.

[13] M. Kim, A. Habiba, J. M. Doherty, J. C. Mills, R. W. Mercer, and J. E. Huettner, "Regulation of mouse embryonic stem cell neural differentiation by retinoic acid," *Developmental Biology,* vol. 328, pp. 456-471, Apr 2009.

[14] K. M. Guan, H. Chang, A. Rolletschek, and A. M. Wobus, "Embryonic stem cell-derived neurogenesis - Retinoic acid induction and lineage selection of neuronal cells," *Cell and Tissue Research,* vol. 305, pp. 171-176, Aug 2001.

[15] Y. H. Jeong, C. H. Park, S. H. Choi, S. H. Lee, H. S. Kim, and Y. H. Suh, "Dehydroevodiamine-HCL extracted from Evodia Rutaecarpa Bentham prevents impairment of learning and memory and neuronal loss," *Journal of Neurochemistry,* vol. 90, pp. 142-142, Aug 2004.

[16] J. F. Liao, W. F. Chiou, Y. C. Shen, G. J. Wang, and C. F. Chen, "Anti-inflammatory and anti-infectious effects of Evodia rutaecarpa (Wuzhuyu) and its major bioactive components," *Chinese Medicine,* vol. 6, p. 8, 2011.

[17] J. H. Peng, C. E. Zhang, W. Wei, X. P. Hong, X. P. Pan, and J. Z. Wang, "Dehydroevodiamine attenuates tau hyperphosphorylation and spatial memory deficit induced by activation of glycogen synthase kinase-3 in rats (vol 52, pg 1521, 2007)," *Neuropharmacology,* vol. 59, pp. 654-654, Dec 2010.

[18] S. Breslin and L. O'Driscoll, "Three-dimensional cell culture: the missing link in drug discovery," *Drug Discovery Today,* vol. 18, pp. 240-249, Mar 2013.

[19] A. S. Ribeiro, E. M. Powell, and J. B. Leach, "Neural Stem Cell Differentiation in 2D and 3D Microenvironments," in *26th Southern Biomedical Engineering Conference, SBEC 2010,* Univ Maryland, College Park, MD, 2010, pp. 422-425.

[20] C. Godugu, A. R. Patel, U. Desai, T. Andey, A. Sams, and M. Singh, "AlgiMatrix (TM) Based 3D Cell Culture System as an In-Vitro Tumor Model for Anticancer Studies," *Plos One,* vol. 8, p. 13, Jan 2013.

[21] W. H. Suh, Ananthanarayanan, Badriprasad, Tirrell, Matthew, "Molecular Engineering of Peptides for Cellular Adhesion Control," ed John Wiley & Sons, Inc., 2013.

[22] H. G. Cui, M. J. Webber, and S. I. Stupp, "Self-Assembly of Peptide Amphiphiles: From Molecules to Nanostructures to Biomaterials," *Biopolymers,* vol. 94, pp. 1-18, Jan 2010.

[23] B. F. Lin, K. A. Megley, N. Viswanathan, D. V. Krogstad, L. B. Drews, M. J. Kade, *et al.*, "pH-responsive branched peptide amphiphile hydrogel designed for applications in regenerative medicine with potential as injectable tissue scaffolds," *Journal of Materials Chemistry,* vol. 22, pp. 19447-19454, 2012.

[24] H. Lee, J. Rho, and P. B. Messersmith, "Facile Conjugation of Biomolecules onto Surfaces via Mussel Adhesive Protein Inspired Coatings," *Advanced Materials,* vol. 21, pp. 431-+, Jan 2009.

[25] D. Missirlis, D. V. Krogstad, and M. Tirrell, "Internalization of p53(14-29) Peptide Amphiphiles and Subsequent Endosomal Disruption Results in SJSA-1 Cell Death," *Molecular Pharmaceutics,* vol. 7, pp. 2173-2184, Nov-Dec 2010.

[26] P. V. Finotelli, D. A. Sampaio, M. A. Morales, A. M. Rossi, and M. H. Rocha-Leao, "Ca ALGINATE AS SCAFFOLD FOR IRON OXIDE NANOPARTICLES SYNTHESIS," *Brazilian Journal of Chemical Engineering,* vol. 25, pp. 759-764, Oct-Dec 2008.

[27] R. Langer, "Drug delivery and targeting," *Nature,* vol. 392, pp. 5-10, Apr 1998.

[28] R. T. Patil and T. J. Speaker, "Retention of trypsin activity in spermine alginate microcapsules," *Journal of Microencapsulation,* vol. 14, pp. 469-474, Jul-Aug 1997.

[29] H. H. Tonnesen and J. Karlsen, "Alginate in drug delivery systems," *Drug Development and Industrial Pharmacy,* vol. 28, pp. 621-630, 2002.

[30] K. Y. Lee and D. J. Mooney, "Alginate: Properties and biomedical applications," *Progress in Polymer Science,* vol. 37, pp. 106-126, Jan 2012.

[31] M. Shachar, O. Tsur-Gang, T. Dvir, J. Leor, and S. Cohen, "The effect of immobilized RGD peptide in alginate scaffolds on cardiac tissue engineering," *Acta Biomaterialia,* vol. 7, pp. 152-162, Jan 2011.

[32] J. A. Burdick, C. Chung, X. Q. Jia, M. A. Randolph, and R. Langer, "Controlled degradation and mechanical behavior of photopolymerized hyaluronic acid networks," *Biomacromolecules,* vol. 6, pp. 386-391, Jan-Feb 2005.

[33] J. A. Burdick and G. D. Prestwich, "Hyaluronic Acid Hydrogels for Biomedical Applications," *Advanced Materials,* vol. 23, pp. H41-H56, Mar 2011.

[34] P. M. Kharkar, K. L. Kiick, and A. M. Kloxin, "Designing degradable hydrogels for orthogonal control of cell microenvironments," *Chemical Society Reviews,* vol. 42, pp. 7335-7372, 2013.

[35] S. K. Seidlits, Z. Z. Khaing, R. R. Petersen, J. D. Nickels, J. E. Vanscoy, J. B. Shear*, et al.*, "The effects of hyaluronic acid hydrogels with tunable mechanical properties on neural progenitor cell differentiation," *Biomaterials,* vol. 31, pp. 3930-3940, May 2010.

[36] M. A. Green, L. E. Bilston, and R. Sinkus, "In vivo brain viscoelastic properties measured by magnetic resonance elastography," *Nmr in Biomedicine,* vol. 21, pp. 755-764, Aug 2008.

[37] C. Vogel and E. M. Marcotte, "Insights into the regulation of protein abundance from proteomic and transcriptomic analyses," *Nature Reviews Genetics*, vol. 13, pp. 227-232, Apr 2012.